Journal of Low Temperature Physics (2020) 199:416–424
https://doi.org/10.1007/s10909-019-02314-3

The Cryogenic AntiCoincidence Detector for ATHENA X-IFU: The Project Status

C. Macculi[1] · A. Argan[1] · D. Brienza[1] · M. D'Andrea[1] · S. Lotti[1] · G. Minervini[1] · L. Piro[1] · M. Biasotti[2] · L. Ferrari Barusso[2] · F. Gatti[2] · M. Rigano[2] · G. Torrioli[3] · M. Fiorini[4] · S. Molendi[4] · M. Uslenghi[4] · E. Cavazzuti[5] · A. Volpe[5]

Received: 17 July 2019 / Accepted: 13 December 2019 / Published online: 7 January 2020

Abstract

The ATHENA observatory is the second large class ESA mission to be launched on 2031 at L2 orbit. One of the two onboard instruments is X-IFU, a TES-based kilo-pixel array able to perform simultaneous high-grade energy spectroscopy (FWHM 2.5 eV@7 keV) and imaging over the 5′ field of view. The X-IFU sensitivity is degraded by primary particle background of both solar and galactic cosmic ray (GCR) origins, and by secondary electrons produced by primaries, interacting with the materials surrounding the detector: These particles cannot be distinguished by the scientific photons, thus degrading the instrument performance. Results from studies regarding the GCR component performed by Geant4 simulations address the necessity to use background reduction techniques to enable the study of several key science topics. This is feasible by combining an active Cryogenic AntiCoincidence detector (CryoAC) and a passive electron shielding to reach the required residual particle background of 0.005 cts/cm^2/s/keV inside the 2–10 keV scientific energy band. The CryoAC is a four-pixel detector made of Si-suspended absorbers sensed by a network of IrAu TESes and placed at a distance < 1 mm below the TES array. Here we will provide an overview of the CryoAC program, starting with some details on the background assessment having impacts on the CryoAC design; then, we continue with its design concept including electronics and the Demonstration Model results, to conclude with programmatic aspects.

Keywords ATHENA X-IFU · Anticoincidence detectors · TES

✉ C. Macculi
claudio.macculi@inaf.it

[1] INAF/IAPS, Rome, Italy

[2] Department of Physics, University of Genova, Genoa, Italy

[3] CNR/IFN, Rome, Italy

[4] INAF/IASF, Milan, Italy

[5] ASI, Rome, Italy

1 Introduction

The ATHENA mission [1] has been conceived to provide exhaustive answers to the following astrophysical questions: How does ordinary matter assemble into the large-scale structures we see today? How do black holes grow and shape the universe? The result is a satellite having two onboard complementary instruments: the X-IFU [2] and the WFI [3]. The X-IFU will provide: (a) 3D integral field spectroscopic mapping of hot cosmic plasmas, enabling measurements of gas bulk motions and turbulence, chemical abundances and the spatial distribution of these and other physical parameters; (b) weak spectroscopic line detection, enabling the detection of unresolved absorption and emission lines from warm and hot intergalactic medium filaments and weak spectral features produced by unusual ion species or states; (c) physical characterization of the Hot and Energetic Universe, including plasma diagnostics using emission line multiplets, AGN reverberation and black hole spin measurements, winds in galactic sources in outburst, AGN winds and outflows, stellar outflows, solar wind charge exchange, etc. The WFI in the survey mode will provide: (a) the access to a new discovery space for supermassive black holes; (b) the identification of distant galaxy groups and clusters, thus allowing to measure their gas entropy profiles on all mass scales out to $z \sim 2$; and (c) temperature maps of clusters around radio-loud AGN out to intermediate redshifts. It will also map shock structures, will test jet evolution models and will infer their impact at the epoch of group and cluster formation.

In particular, one of the X-IFU scientific aims, the reference instrument along this paper, is to provide high-spectral-energy-resolution maps of faint or diffuse sources; thus, a very low-residual-particle background (bkg) is required around the TES array detector. To perform this task, it is necessary to adopt reduction techniques. So, the cryogenic X-IFU focal plane assembly (FPA) will be equipped with a passive electron shielding surrounding the TES array and an active anticoincidence detector as the CryoAC. On February 2019, the I-PRR (Instrument Preliminary Requirement Review) for X-IFU has been held, where we reported the CryoAC instrument definition, its design concept and related trade-off studies. At the adoption planned on 2021, it is requested by ESA that critical subsystems must reach TRL5 (Technology Readiness Level) by Demonstration Model (DM) to enable critical technologies.

2 From BKG Assessment to the CryoAC Design Concept

2.1 BKG Assessment

In high-energy astrophysics, the particle bkg assessment is a typical task to be pursued during Phase A of an ESA space mission lifecycle. It directly affects the instrument sensitivity; hence, for the instrument design, the higher the residual bkg, the lower the instrument sensitivity. The requirement foresees a residual bkg

of 0.005 cts/cm^2/s/keV in 2–10 keV scientific energy band. The contribution to the bkg is mainly divided into two categories:

(1) the so-called soft proton/ions ($E <$ few hundred's keV) components, whose origin is the Sun and L2 (present baseline orbit) magnetotail, that can be collimated by the ATHENA grazing incidence X-ray optics toward the FPA
(2) the GCRs (hundred's MeV to GeV) that crossing the satellites over 4π sr arrive at the focal plane producing also secondaries.

While for the low-energy component the plan is to use a magnetic diverter to cut away this flux of charged particles from the cryostat, to reduce the high-energy GCR component it is necessary to adopt an active detection system. We remind that minimum ionizing particles (MIPs), having GeV energy scale, typically deposit ~ 4–5 keV inside the X-IFU scientific energy band. (The TES array absorbers are made of Bi 4.2 μm thick and Au 1.7 μm thick.) To assess the impact of the particle environment onto the TES array, simulations by Monte Carlo method using the Geant4 toolkit have been performed [4, 5]: This primary flux interacts with the "mass model" of the payload, which is a simplified instrument environment, but representative of the mass composition and distribution around the TES array detector (from the satellite, through the cryostat, down to the detailed cryogenic FPA), to produce the expected bkg. In Fig. 1, we show the present X-IFU mass model and the expected residual bkg by applying both reduction techniques. The electron liner made of a Kapton/Bi bilayer, to be revised in the next phase in Kapton/Au due to manufacturing problem when handling the bismuth, is a passive shield necessary to reduce the e^- contribution toward the TES array. It has a two aims: it reduces secondary electrons produced by primaries crossing the niobium magnetic shield (in blue), and it also generates a lower number of tertiary electrons. Moreover, without the CryoAC detector, the TES array would experience a particle bkg ~ 40 higher than the requirement.

2.2 Design Concept

Main requirements and system constraints sizing the CryoAC are given in Table 1:

The main top requirements for which the CryoAC has to be compliant are: (1) the efficiency, having a direct impact onto the low-energy threshold; (2) the dead time, having a direct impact on the detector maximum energy and its time constants, and the power dissipation via the thermal conductance.

Since the CryoAC absorber is based on Si working at sub-K temperatures, the dynamic of pulse evolution after energy deposition will be led by the thermal and athermal regime. Ballistic athermal phonons can soon enter the TESes deposited on the crystal surface, quickly heating the electron gas, thus forming a first pulse. Then, the diffusive phonons will rise generating an added thermal pulse. Athermals are used as flag to rise the particle veto, thus asking for good collection for better pulse shaping. The baseline design is based on absorbers made of a thin Si crystal (0.5 mm thick), where the energy deposited by particles is sensed by a network

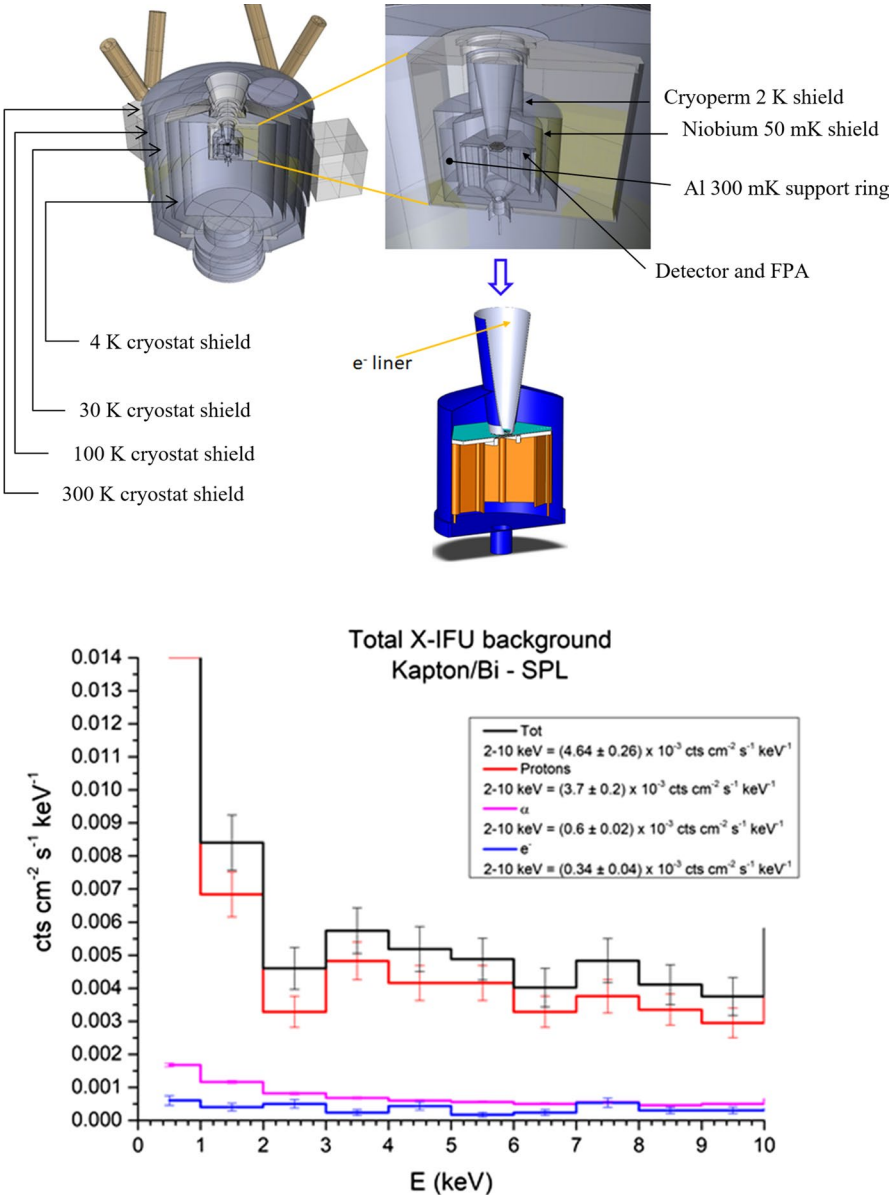

Fig. 1 *Top and center*: X-IFU mass model. On *top left*, complete cryostat, on *top right* a zoom of the FPA region to highlight the detector hexagon in the center. In the *middle* a sketch to show the electron liner shield. *Bottom*: expected residual background from the different particle species present in L2. The requirement is 0.005 cts/cm^2/s/keV (error is due to statistics, and the equivalent time of the simulations is several thousands of seconds) (Color figure online)

Table 1 Main requirements and system constraints sizing the CryoAC

Parameter	Value
Geometrical rejection efficiency	98.5%
Detection efficiency	99.98%
Allocated power dissipation	< 40 nW (CBE)
Time tagging accuracy	≤ 10 μs
Intrinsic dead time	1%

CBE current best estimate

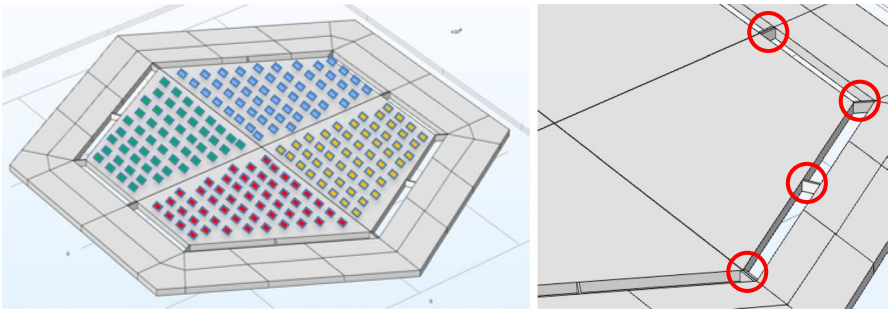

Fig. 2 CryoAC baseline configuration: four independent pixels. It is shown only the "concept": four independent TES networks, each network deposited on a separate trapezoidal absorber. Other details, for example wiring and pad layout, are not shown since they are still under study. On the right, the four silicon beams connecting each of the four absorbers to the silicon rim are shown (Color figure online)

of TES sensors (Fig. 2). The CryoAC is placed below the TES arrays, at a distance < 1 mm. The active part covers a full area of 4.91 cm^2, larger than the TES array (2.3 cm^2).

The baseline detector is divided into four independent pixels; each one has an area of 1.23 cm^2 and has an onboard network of ~ 120 IrAu TES connected in parallel. Each pixel is connected to a gold-plated Si rim by four Si beams, realizing the pixel thermal conductance. Each pixel absorber will also have deposited onboard Pt heaters to increase its temperature, if necessary, to decrease bias currents, thus limiting magnetic coupling effects to the TES array (expected ~ 10 mA order due to the TES network high critical current). The compliance of the design to the requirements has been verified through an analysis of the system, including background assessment by Geant4 [4, 5] and tests on prototypes [6–9]. At present, the baseline design which is the four-pixel detector is being traded off with a monolithic hexagonal absorber to see pro and cons in terms of detector responsivity, rejection efficiency, dead time and robustness.

As for the electronics (Fig. 3), the CryoAC will be read out using four SQUID channels in standard flux-locked-loop configuration (FLL), one for each of the four pixels.

To be compliant with the failure management philosophy, we have adopted as baseline an independent FLL chain for each "pixel + SQUID" that will be served by

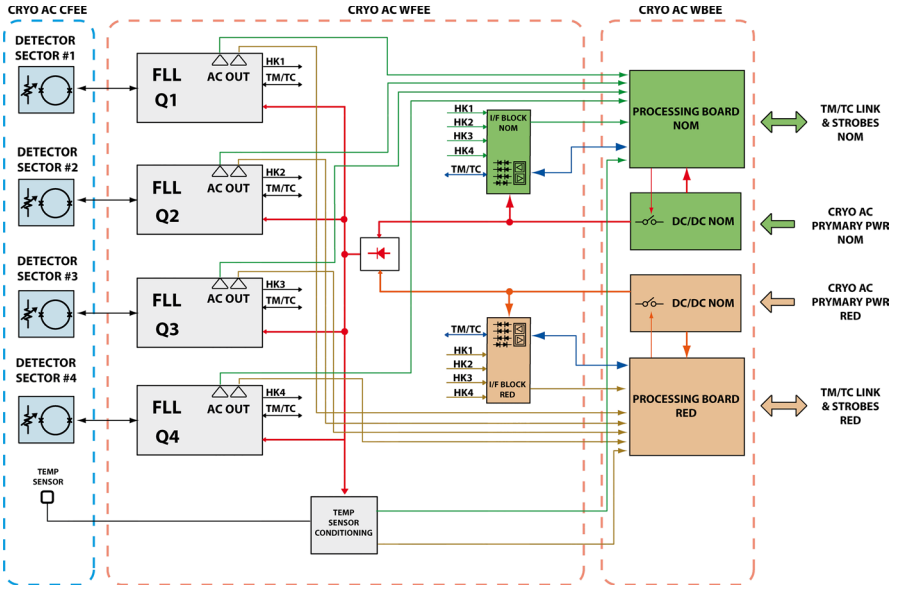

Fig. 3 CryoAC Electronics: Cold Front End (CFEE) composed by the four SQUID to sense the current from the four pixels, Warm Front End divided into four quadrants, each one providing bias to TES and SQUID single pixel and producing the analogic scientific signal (AC OUT) and the FLL housekeeping. On the right, the Warm Back End divided into nominal and redundant boards, each one processing and digitizing the signal from the WFEE and packeting the data to be sent to the instrument control unit (Color figure online)

a so-called quadrant service electronic section inserted in the CryoAC Warm Front End Electronics (WFEE). The Warm Back End Electronics (WBEE) will manage the WFEE, digitize its analogic output, apply quality grades and time stamps to the pulses, and organize the telemetry packet. The baseline plans veto operation on ground due the expected low telemetry rate.

3 CryoAC Fabrication Process

In the context of the DM, as expected for the TRL4 path whose definition is "Component and/or breadboard functional verification in laboratory environment," care has been taken during all the fabrication processes (see Ref. [10] for details) (Fig. 4) that are propaedeutic for all the models to be produced (i.e., engineering model—EM, qualification model—QM and flight model—FM).

Particular attention has been put on the deposition of the IrAu defining the TES critical temperature and the final etching of the chip. Here is a quick description of such processes step by step: (1) silicon wafer, (2) IrAu (240 nm/80 nm thick) bilayer deposition by pulsed laser deposition technique, (3) TES IrAu bilayer etching by ion milling, (4) Pt heater (50 nm thick) fabrication by evaporation and liftoff, (5) Au thermalization layer (~230 nm thick) deposition on rim by evaporation and liftoff, (6) niobium wiring (lower strip) fabrication by RF sputtering and liftoff, (7) silicon oxide insulation by

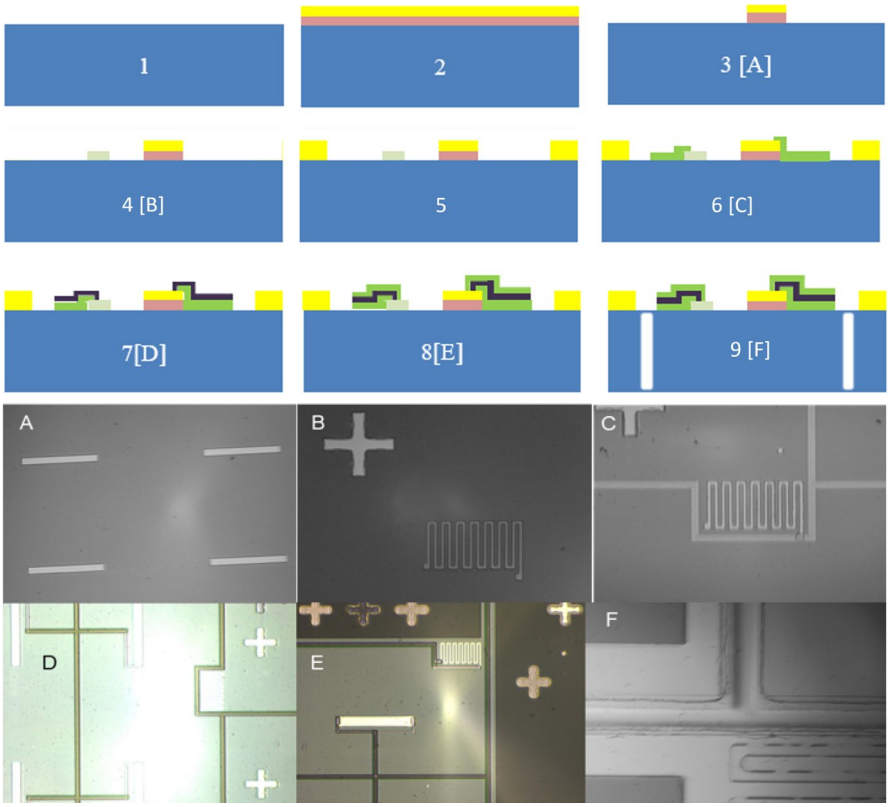

Fig. 4 Fabrication process. See text for details (Color figure online)

evaporation and liftoff, (8) niobium wiring (upper strip) fabrication by evaporation and liftoff, and (9) deep reactive ion etching (first step—Al hard mask deposition; second step—etching using Bosch process; and third step—removal of aluminum mask). To summarize, we have in total seven photolithographic processes: one positive photolithography and etching, and six negative photolithography and liftoff.

It is worth noticing that Nb wiring (lower strip line ~ 490 nm and upper strip line ~ 1000 nm thick, respectively) has been overlapped in anti-inductive configuration to reduce magnetic coupling toward the TES array. The formalization of the procedures in detail is in progress, together with the revision process aimed at ensuring maximum reproducibility and at maximizing the production yield.

4 The DM CryoAC

The aim of the DM (for details see [10, 11]) is the detector functional qualification to get the TRL4, thus consolidating the path to get TRL5 consisting on the "Component and/or breadboard validation in relevant environment." Being the CryoAC

a cryogenic detector, in addition to the usual thermal cycles (cooling and warming up), in the ATHENA context "relevant environment" means to test the CryoAC under mechanical vibration. The DM detector is representative of the baseline, and it is aimed at demonstrating the maturity level of the most critical technology by means of:

- qualification of the manufacturing processes (see Ref. [10] for some details)
- full knowledge of the physics ruling the detector performance (see Refs. [6–11] for details)

Once the DM program will be concluded, the next step is to vibrate the full geometry (see Fig. 2) to get TRL5.

The functional requirements to be satisfied by the DM CryoAC are: suspended pixel size (abs. area) of 1 cm^2; low-energy threshold at 20 keV; operation at

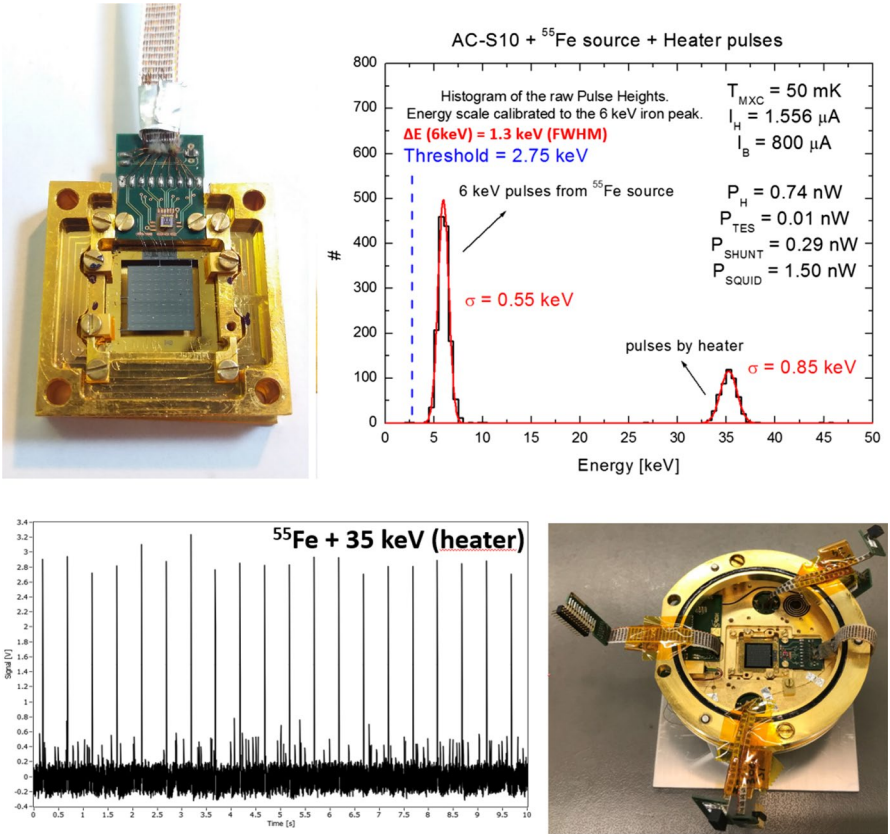

Fig. 5 *Top left* DM CryoAC in INAF holder. *Top right* Energy spectrum from ^{55}Fe and 35 keV pulses injected by the heater. *Bottom left* Raw data stream. *Bottom right* Fit checking in the 40 PxlB flange at SRON (credits SRON) (Color figure online)

$T_b = 50$ mK; and power dissipation < 40 nW. In Fig. 5 are reported some pictures and results of the AC-S10 sample that, being compliant with the DM requirement, has been defined as the "DM CryoAC."

The results are compliant with the requirements. They also show a very low-energy threshold (< 3 keV) and some spectroscopic capability ($\sim 20\%$@6 keV). After the stand-alone test performed in Italy, the DM has been delivered to SRON for integration at the chipset level with the TES array.

5 Near-Term CryoAC Activities

The main near-term milestones are: production of a first structural model (SM) to be vibrated by Fall 2019, thus having a feedback on the Si beams, defining the absorber-to-bath thermal conductance, from the robustness point of view; the closure of a proto-EM design (a propaedeutic model for the EM) by the end of 2019 which is a detector having hexagonal geometry (see Fig. 2), but only one instrumented readout chain, to start its production in early 2020. By mid-2020, the production of a second SM to get TRL5 with respect to the first one will have representative interfaces to the FPA. We are working to produce a Warm Electronics breadboard to be tested in combination with the proto-EM by the end of 2020: The coupling of these two items is the base for the EM CryoAC design. By the end of 2021, we expect to close the work related to an end-to-end simulator whose main driver is the pulse production, starting from the athermal and thermal phonon physics, to be used as design tool for the electronics (trigger logic, pileup and dead time).

Acknowledgements This work has been supported by ASI Contract No. 2018-11-HH.0, ESA CTP Contracts Nos. 4000116655/16/NL/BW and 4000114932/15/NL/BW, and by AHEAD H2020 project (Grant No. 654215). SRON is acknowledged for the fit-checking picture.

References

1. K. Nandra, X. Barcons, D. Barret, A. Fabian, J.W. den Herder, L. Piro, M. Watson et al., *ATHENA mission proposal* (2013). https://www.the-ATHENA-x-ray-observatory.eu/images/ATHENAPapers/The_ATHENA_Mission_Proposal.pdf. Accessed 21 Dec 2019
2. D. Barret, T. Lam Trong, J.W. den Herder, L. Piro, M. Cappi et al., Proc. SPIE **10699**, 106991G (2018). https://doi.org/10.1117/12.2312409
3. N. Meidinger, J. Eder et al., Proc. SPIE **9905**, 99052A (2016). https://doi.org/10.1117/12.2231604
4. S. Lotti et al., Proc. SPIE **10699**, 106991Q (2018). https://doi.org/10.1117/12.2313236
5. S. Lotti et al., XIFU-INAF-BKG-TN-0002. Internal Technical Note (2019)
6. C. Macculi et al., Proc. SPIE **9144**, 91445S (2014). https://doi.org/10.1117/12.2054946
7. M. D'Andrea et al., Proc. SPIE **9905**, 99055X (2016). https://doi.org/10.1117/12.2231412
8. M. D'Andrea et al., J. Low Temp. Phys **193**, 949 (2018). https://doi.org/10.1007/s10909-018-2039-4
9. M. D'Andrea et al., Proc. SPIE **10699**, 106994T (2018). https://doi.org/10.1117/12.2313280
10. M. Biasotti, J. Low Temp. Phys. (2019) (**under review**)
11. M. D'Andrea, J. Low Temp. Phys. (2019). https://doi.org/10.1007/s10909-019-02300-9